Polarity Reversal of Terahertz Waves Radiated from Semi-insulating InP Surfaces Induced by Temperature

doi: 10.1103/PhysRevB.67.195308

Polarity reversal of terahertz waves radiated from semi-insulating InP surfaces induced by temperature

M. Nakajima* and M. Hangyo
Research Center for Superconductor Photonics, Osaka University, 2-1 Yamadaoka, Suita, Osaka 565-0871, Japan

M. Ohta† and H. Miyazaki
Department of Applied Physics, Tohoku University, Sendai 980-8579, Japan
(Received 13 August 2002; published 7 May 2003)

The temperature dependence of the terahertz (THz) radiation from semi-insulating InP surfaces excited by ultrashort laser pulses has been studied in detail between 10 and 300 K. It is found that the electric field of the radiated THz waves show opposite polarity at low and high temperatures for low-density excitation. The temperature dependence is explained by the competing model of the drift and the diffusion currents. Good agreement between the experimental results and the calculations based on the drift-diffusion model shows that the dominant radiation mechanism is the current surge effect due to the surface electric field at high temperatures and the photo-Dember effect at low temperatures.

DOI: 10.1103/PhysRevB.67.195308 PACS number(s): 78.47.+p, 42.65.Re, 78.68.+m

I. INTRODUCTION

Terahertz (THz) radiation from semiconductor surfaces excited by ultrashort laser pulses has attracted much attention because it is used as a THz radiation source for various applications and it provides other important information on the ultrafast dynamics of nonequilibrium carrier transport as compared to conventional methods.[1–10] Studies on the applications of THz waves such as THz time-domain spectroscopy (THz-TDS) and imaging have been actively conducted.[5–8] Recently, the ultrafast dressing process of the charged particles in GaAs was clarified by analyzing the THz wave forms.[8] Detecting THz waves emitted from semiconductor surfaces, which provides information not only on the amplitude but also on the phase, enables the direct acquisition of information on nonequilibrium carrier transport with a femtosecond time scale and some such studies have been reported.[5,9,10] Hu *et al.* and Leitenstorfer *et al.* have directly observed the processes of the instantaneous polarization, ballistic transport, carrier drift, and velocity overshoot in GaAs by observing THz wave forms.[9,10]

THz radiation is understood as the emission from a small electric dipole antenna induced by optical pulse excitation. The electric field E_{THz} of THz radiation in the far field is given by

$$E_{\mathrm{THz}}(t) \propto \frac{dJ(t)}{dt}, \tag{1}$$

where J is the transient current induced by the optical pulse excitation. Equation (1) shows that the amplitude E_{THz} depends on the time derivative of J and the polarity of the THz wave is determined by the direction of J. The current surge effect driven by the surface electric field was proposed as a THz radiation mechanism for wide band-gap semiconductors such as GaAs. The photoinjected electrons and holes are accelerated in opposite directions by the surface electric field, causing the drift current (J_{drift}) to flow.[3,4] There is another mechanism related to the optical generation of carriers, that is, buildup of the Dember field due to the diffusion current (J_{diffus}) associated with photogenerated electrons and holes.[11] It is reported that the emission of THz waves from the surface of narrow band-gap semiconductors, which have weak surface electric fields, is due to the photo-Dember effect.[12] Very recently, Johnston *et al.* reported a theoretical study about THz radiation from GaAs and InAs surfaces.[13] They showed that the radiation process for GaAs is primarily the current surge effect while for InAs, the photo-Dember effect is primary. For the high-density excitation case, optical rectification was reported as the THz radiation mechanism, which is associated with instantaneous polarization by the nonlinear optical effect.[14,15] These radiation mechanisms coexist and their relative contribution is governed by the type of materials and the excitation conditions.

In this work, we report the crossover of the dominant radiation mechanisms from the current surge effect to the photo-Dember effect for semi-insulating (SI) InP with decreasing temperature from room temperature to 10 K. We have used Fe-doped SI InP with a (100) surface as a sample. SI InP has a weak surface electric field compared to *n*- and *p*-type InP although it is a wide band-gap semiconductor as GaAs. To date, the enhancement of the radiation power with decreasing temperature was reported for some semiconductors and this is mainly explained by the temperature variation of the static electron mobility.[1–4,16–18] The shape change of THz wave forms with temperature for InSb has been reported by Hu *et al.* and they proposed that it is due to the changes of the depletion width and complex conductivity with temperature.[2] For the case of optical rectification, polarity reversal of THz radiation with temperature has been reported for GaAs when the excitation laser energy is close to the band-gap energy.[4] This result is interpreted by the sign change of the second-order susceptibility for optical rectification due to the change of band-gap energy with temperature.

We have studied the temperature dependence of THz radiation from SI-InP surfaces for low- and high-density excitation in detail. The polarity reversal of the THz wave form

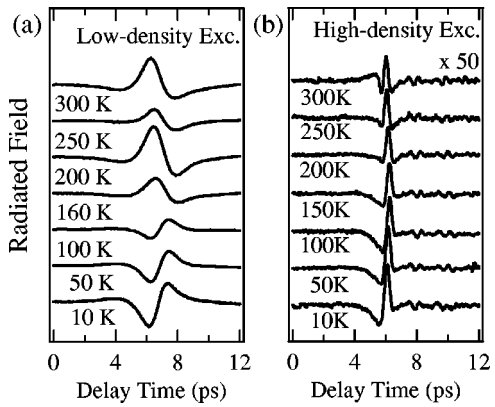

FIG. 1. The wave forms of THz radiation from a SI-InP surface at various temperatures for (a) low-density excitation and (b) high-density excitation.

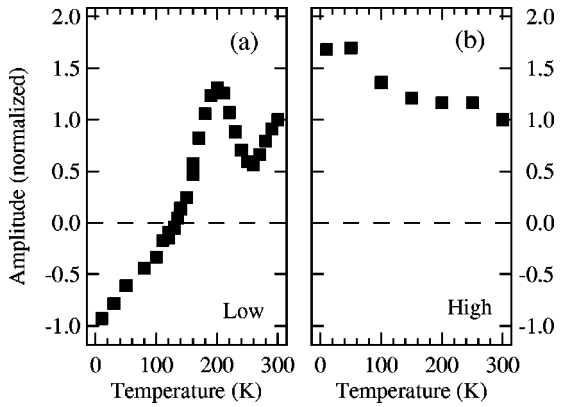

FIG. 2. Temperature dependence of the peak amplitude at ~6 ps in Fig. 1 for (a) low-density excitation and (b) high-density excitation.

is observed at ~140 K for low-density excitation. We discuss this temperature dependence based on the drift-diffusion model and demonstrate that the dominant radiation mechanism changes from the current surge effect at high temperatures to the photo-Dember effect at low temperatures.

II. EXPERIMENT

A pump and probe technique was used in the measurement. A mode-locked Ti:sapphire laser delivered ultrashort light pulses of 100-fs duration with a central photon energy of 1.55 eV at a pulse repetition rate of 82 MHz. The excitation energy was higher than the band-gap energy of InP (1.42 eV at 1.6 K) (Ref. 19) at all temperatures of the measurement (10–300 K). The focused and unfocused pump pulses excited the sample in a He-flow-type cryostat. The angle of incidence was 45° with respect to the surface normal and the excitation density (I_{exc}) on the sample surface was ~1 W/cm^2 for low-density excitation and ~10^3 W/cm^2 for high-density excitation. The THz wave radiated from the sample surface passed through the quartz window of the cryostat and it was focused on a photoconductive antenna of a detector by a pair of off-axis paraboloidal mirrors. The THz electric field was detected by a dipole-type low-temperature-grown (LT) GaAs photoconductive antenna.[20] The electric field of the THz wave was detected by the photoconductive antenna which was triggered by optical probe pulses with variable time delay. The detection frequency width of the experimental system was estimated to be ~3 THz, which corresponds to the time resolution of ~300 fs, from the experimental results for high-density excitation stated later in the paper.

III. EXPERIMENTAL RESULTS AND DISCUSSION

Figures 1(a) and 1(b) show the wave forms radiated from SI InP at various temperatures for low-density excitation (I_{exc}~1 W/cm^2) and high-density excitation (I_{exc} ~10^3 W/cm^2), respectively. The vertical scale in Fig. 1(b) is expanded 50 times as compared to that in Fig. 1(a). It is clearly seen from these figures that the temperature dependence for low- and high-density excitation cases is quite different. Especially, the wave forms for low-density excitation have opposite polarities at low and high temperatures, while those for high-density excitation have the same polarity throughout all temperatures. It is seen that the widths of the wave forms in Fig. 1(b) are apparently narrower than those in Fig. 1(a). This fact indicates that the observed radiation for the high-density excitation case originates from the optical rectification effect, in which the process occurs almost instantaneously.[14,15] This was confirmed by measuring the azimuthal angle dependence of the radiation amplitude at room temperature for the high-density excitation case. The temperature dependence of the peak amplitude at approximately ~6 ps in Fig. 1 is plotted in Fig. 2. It is confirmed that the temperature dependencies of the square of the peak amplitude as shown in Figs. 2(a) and 2(b) almost agree with those of the radiated power obtained by numerically integrating the square of the radiation amplitude in the time domain. It is seen in Fig. 2(a) that the polarities of the wave forms show opposite signs above and below 140 K and the amplitude becomes very small at 140 K. With increasing temperature from 10 to 140 K, the peak amplitude decreases and the polarity reversal occurs at 140 K. By increasing temperature further, the peak amplitude increases until it reaches a maximum at 200 K, decreases, shows a dip at ~250 K, and then increases again. This temperature dependence is considerably different from that reported for other semiconductors.[1–4,16,17] According to previous reports, THz radiation intensity increases monotonically with decreasing temperature and this is explained by the increase of the electron mobility at low temperatures. However, our results at low-density excitation that the polarity reversal occurs at 140 K and the amplitude decreases with decreasing temperature from 300 K cannot be explained only by the effect of the electron mobility. In the paper by Hu *et al.*,[2] a change of the wave form radiated from the *n*-type InSb surface with temperature has been reported. The polarity changes with temperature, but the change of the shape occurs continuously. They reported that the absolute value of the amplitude increases monotonically with decreasing temperature and does not show a minimum at some temperature. This is very different from our results. They interpreted this result as the

change of the complex conductivity with temperature, which affects the frequency-dependent transmittance of the THz wave from the sample to free space. In contrast, the absolute value of the amplitude becomes very small at ~140 K in our case, corresponding to the polarity reversal. This minimum at ~140 K cannot be explained by the change of the complex conductivity because the transmittance of the THz wave, which depends on the free-carrier density, is expected to increase monotonically due to the decrease of free-carrier density with decreasing temperature. The effect of complex conductivity with temperature is ruled out in our case because the free-carrier density in SI InP is very small as compared to InSb and the change of the free-carrier density with temperature hardly affects the transmittance of the THz wave. Actually, we measured the temperature dependence of the transmittance of the THz wave in SI InP by using the THz-TDS technique. The results show that there is no significant temperature dependence of the transmittance and the frequency dependence of the transmittance is flat below 1 THz below 300 K. The peak amplitude for high-density excitation in Fig. 2(b) decreases monotonically with increasing temperature. This dependence agrees with the results of previous work by Zhang and Jin.[4] The enhancement at low temperatures shown in Figs. 1(b) and 2(b) has been explained by the increase of dephasing time.[4] The spectrum (not shown) for high-density excitation extends to ~3 THz, which should be limited by the detection width of the experimental system, while that for low-density excitation extends to ~1 THz. The spectral shape for high-density excitation shows almost no temperature dependence while that for low-density excitation shows a small but abrupt change at 140 K. The widths of the spectra below 140 K are slightly broad compared to those above 140 K. These experimental results indicate that the radiation mechanism of the THz wave is different at low- and high-density excitations. It is confirmed that optical rectification is the dominant radiation process for high-density excitation from the azimuthal angle dependence as stated before. At low-density excitation, the radiated waves show opposite polarity at low and high temperatures, and the radiation process as well as the temperature dependence for low-density excitation is discussed in relation to the photogenerated carrier dynamics below.

The temperature dependence of THz radiation for *n*- and *p*-type InP, the carrier densities of which at room temperature are 2.5×10^{18} and 5.7×10^{18} cm^{-3}, respectively, at low-density excitation was measured for comparison. The polarities of the wave forms are opposite for *n*- and *p*-type InP and polarity reversal was not observed for both types in the temperature range from 10 to 300 K. This is explained by the fact that the band bending at the surfaces is upward for *n*-type InP and downward for *p*-type InP. These results indicate that the main radiation mechanism for *n*- and *p*-type InP is the current surge effect due to the surface electric field. It is reported that the band bending at the surface for SI InP is downward as shown in Fig. 3(a), which is the same as *p*-type InP.[21,22] The polarity of the wave form for SI InP above 140 K is the same as that for *p*-type InP, suggesting that the radiation mechanism above 140 K is the current surge effect. To explain the polarity reversal and the temperature dependence in Fig. 1(a), we propose a crossover of the dominant radiation mechanism from the current surge effect at high temperatures (above 140 K) to the photo-Dember effect at low temperatures (below 140 K). According to Eq. (1), the polarity of the THz wave is determined by the direction of *J*, which corresponds to J_{drift} for the current surge effect and J_{diffus} for the photo-Dember effect. Figures 3(a) and 3(b) show the schematic diagram of the flow of J_{drift} and J_{diffus} in SI InP, respectively. J_{drift} flows toward the inner region of the sample due to the surface electric field while J_{diffus} flows toward the sample surface due to the difference of the diffusion speed between electrons and holes. According to this explanation, the polarities of the THz wave form for the current surge effect and the photo-Dember effect are opposite. As stated before, the polarity of the wave form above 140 K is consistent with that expected for J_{drift} and that below 140 K is consistent with J_{diffus}. Enhancement of the radiation amplitude at low temperatures has been reported for InSb for which, the main radiation mechanism is believed to be the photo-Dember effect.[18] For comparison, we measured the temperature dependence of the THz wave radiated from SI GaAs. The polarity reversal is not observed and the peak amplitude decreases as the temperature increases to ~150 K, reaches a minimum, and increases with increasing temperature up to 300 K. The energy band near the surface of SI-GaAs bends upward,[21,22] which is opposite to that for SI InP. In this case, both J_{drift} and J_{diffus} flow toward the sample surface and the polarity reversal of the THz wave cannot occur. The difference of the temperature dependence for SI InP and SI GaAs could be explained by this consideration.

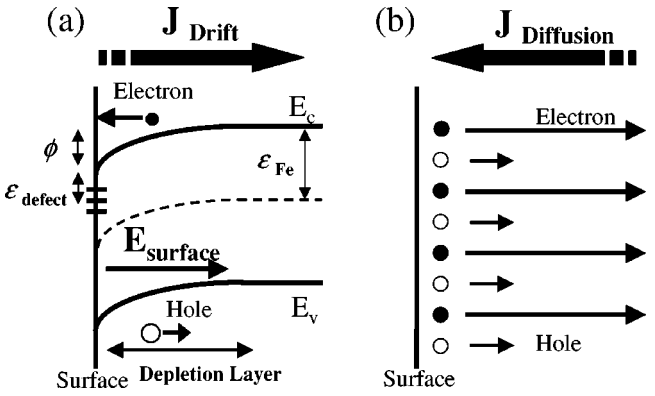

FIG. 3. The schematic flow of (a) the drift current (J_{drift}) and (b) the diffusion current (J_{diffus}) near the surface of SI InP after photoexcitation.

For a more quantitative analysis we conducted a theoretical calculation based on the drift-diffusion model for electrons and holes generated by photoexcitation with a femtosecond time scale.[23,24] This model is the most simple formulation of the Boltzmann transport equation and can be applied when the relaxation-time approximation is valid.[25] It is known that the thermalization of photogenerated carriers occurs with a characteristic time of ~100 fs in our excitation conditions,[26] and this thermalization time is much smaller than the time scale of our calculation. Therefore the drift-

diffusion model is applicable for our calculation. This calculation is based on solving simultaneously the continuity equation of the carriers and Poisson equation:

$$\frac{\partial N_i(z,t)}{\partial t} = G(z,t) + \frac{\partial}{\partial z}\left\{ D_i \frac{\partial N_i(z,t)}{\partial z} \right\} \pm \frac{\partial}{\partial z}\{\mu_i E(z,t) N_i(z,t)\}, \quad (2)$$

$$\frac{\partial E(z,t)}{dz} = \frac{e}{\epsilon_0 \epsilon_s}\{N_h(z,t) - N_e(z,t) - N_a^-(z,t)\}, \quad (3)$$

where $G(z,\ t)$ is the optical generation term, D_i and μ_i ($i = e,\ h$ indicate electrons and holes, respectively) are the diffusion constant and the mobility of the carrier in the Γ valley, respectively, $N_a^-\ (z,\ t)$ is the density of the ionized deep acceptor, and e, ϵ_0, and ϵ_s are the electron charge, the static dielectric permittivity, and the relative dielectric constant. The spatial distribution of the carriers $N_i\ (z,\ t)$ and the electric field $E\ (z,\ t)$ near the surface ($z=0$) were calculated simultaneously. Subsequently, we obtained the radiated THz wave forms E_{THz} from the second time derivative of the dipole moment obtained from $N_i\ (z,\ t)$.

In this calculation, we used the diffusion constant D_i and the mobility μ_i of the carrier at the Γ valley, the photogenerated carrier density, and the static surface electric field $E\ (z,\ 0)$ as parameters which depend on temperature. It is known that the electronic characteristics of the SI semiconductors are strongly affected by the deep donor or acceptor. We used values for which the doping density of the deep Fe acceptor is $10^{17}\ \mathrm{cm}^{-3}$ and its level [ϵ_{Fe} in Fig. 3(a)] is 0.6-eV below the bottom of the conduction band (CB),[27] while the shallow donor density is $10^{15}\ \mathrm{cm}^{-3}$. The maximum electric field E_s (E at the surface) and the depletion width w are given by the Schottky model:[21]

$$E_s = \left(\frac{2eN_s\phi}{\epsilon_0 \epsilon_s} \right)^{1/2}, \quad (4)$$

$$w = \left(\frac{2\epsilon_0 \epsilon_s \phi}{eN_s} \right)^{1/2}, \quad (5)$$

where N_s is the static total carrier density including the ionized deep Fe acceptor, and ϕ is the band-bending energy at the surface. In the Schottky model, $E\ (z,\ 0)$ decreases linearly to zero within w. ϕ corresponds to the difference between the surface and bulk Fermi levels (chemical potential). The surface Fermi level is pinned at the surface defect level [$\epsilon_{\mathrm{defect}}$ in Fig. 3(a)] which is located 0.45-eV below the bottom of CB at all temperatures of the measurement.[22] The temperature dependence of the bulk Fermi level and N_s was calculated using the Schockley plot.[21] The Fermi level is determined so as to satisfy the neutral condition. The calculations show that N_s is fixed to $\sim 10^{15}\ \mathrm{cm}^{-3}$ at all temperatures of the measurement, and the bulk Fermi level at 10 K is located near ϵ_{Fe} and the position shifts to the lower-energy side with increasing temperature up to 300 K. The decrease of the bulk Fermi level corresponds to the increase of ϕ with increasing temperature. These results indicate that the direction of the band bending is downward at all temperatures below 300 K, and exclude the possibility of the reversal of direction of the surface electric field. The calculated temperature dependence of E_s and w is shown in Fig. 4. This figure shows that E_s and w increase with increasing temperature up to 300 K. The values E_s and w are 9.3 kV/cm and 0.64 μm at 300 K, and 6.6 kV/cm and 0.45 μm at 10 K, respectively.

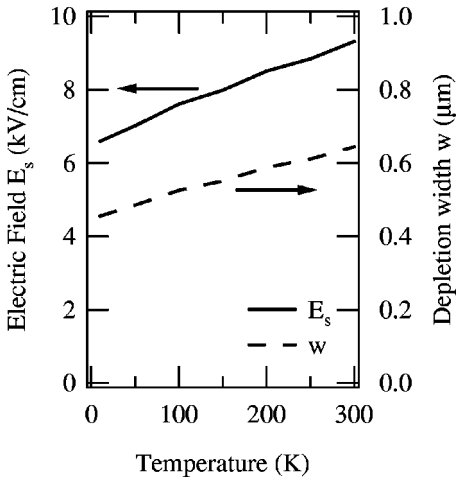

FIG. 4. The calculated temperature dependence of the electric field at surface E_s and depletion width w.

The quantities μ_i and D_i have the relations $\mu_i = e\tau_i / m_i^*$ and $D_i = k_B T_c \tau_i / m_i^*$ (Einstein relation), where τ_i is the scattering time of the photogenerated carrier and m_i^* is the effective mass at the Γ valley. The high carrier temperatures $T_c = 1200$ K at 300 K and $T_c = 700$ K at 10 K were assumed in the time scale of the calculation since the excess energy of the photoexcitation is distributed to the photogenerated carriers. The temperature dependence of τ_i was estimated by using the result of Ref. 28 and it is shown in Fig. 5. The solid and dashed lines show the temperature dependence of τ_e calculated by taking account of the effect of high T_c (τ_e with T_c) and that of τ_e using the lattice temperature as T_c (τ_e without T_c), respectively. The difference between the solid and dashed lines in Fig. 5 at low temperatures, that is, τ_e with T_c increases with decreasing temperature while τ_e without T_c decreases with decreasing temperature below 100 K, is due to the effect of the polar impurity scattering. The scattering time by the polar impurity scattering strongly depends on the carrier energy, corresponding to T_c, and it increases with increasing T_c. The temperature dependence of τ_e with T_c and the peak amplitude of the THz radiation at high-density excitation as shown in Fig. 2(b) are very similar. It was reported that the THz radiation amplitude at high-density excitation depends on the dephasing time.[4] These facts suggest that the THz radiation amplitude is not governed by τ_e without T_c, but it is governed by τ_e with T_c. We used τ_e with T_c as the parameter for our calculation. The value of τ_e at 300 K, which was mainly determined by LO

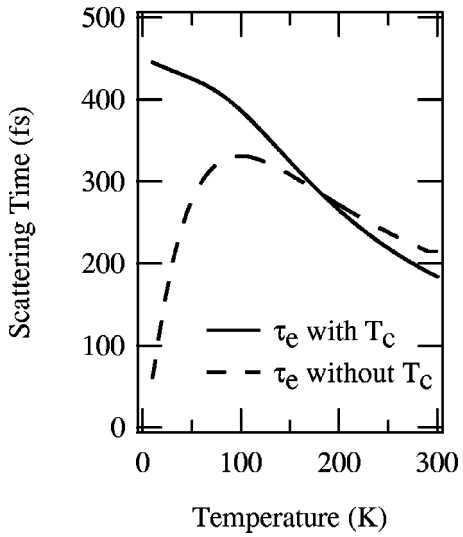

FIG. 5. The calculated temperature dependence of the scattering time of the electron τ_e. The solid and dashed lines show the temperature dependence of τ_e by taking account of the effect of the high T_c (τ_e with T_c) and that of τ_e using the lattice temperature as T_c (τ_e without T_c), respectively.

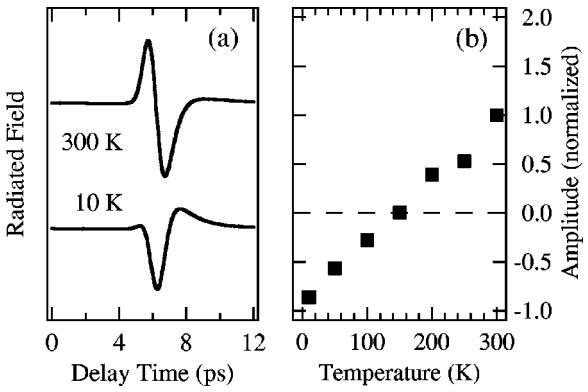

FIG. 6. (a) The THz wave forms at 300 K and 10 K and (b) temperature dependence of the amplitude calculated by the drift-diffusion model.

phonon scattering, was ~180 fs and that at 10 K, which was mainly dominated by neutral impurity scattering, was ~450 fs.

The THz wave radiated from the sample surface passed through the quartz window of the cryostat and it was detected by the photoconductive antenna. The effect of deformations of the THz wave forms by passing through the quartz window was calculated using the complex refractive index of the window for the THz wave obtained by the THz-TDS measurement. The THz electric field detected by the photoconductive antenna was calculated by the convolution of E_{THz} with the response function of the antenna, which is affected by the generation and decay of the photogenerated carriers excited by the probe pulse.[12] The rising shape of the photogenerated carriers was obtained by the time integral of the Gaussian pulse of 100-fs width and the falling shape is assumed to be the exponential with the time constant of 500 fs, which is the carrier lifetime of the LT-GaAs film in the detector obtained by the reflection-type pump-probe measurement. The response function of the antenna such as the impedance and resonance was not considered here.[29]

The calculated THz wave forms at 300 K and 10 K and the temperature dependence of the amplitude are shown in Figs. 6(a) and 6(b), respectively. The resulting calculated wave forms at 300 K and 10 K shown in Fig. 6(a) have different polarities with each other and they reproduce the observed characteristics shown in Fig. 1(a) well. The good agreement between the calculations and the experimental data supports our model that the dominant THz radiation mechanism from the SI InP surface is the current surge effect due to the surface electric field at high temperatures and the photo-Dember effect at low temperatures. The difference in the widths of the wave forms between the experiment and the calculation is attributed to the assumption that we omitted the effect of the impedance and resonance by the antenna structure. However, a certain discrepancy exists between the experiments and the calculations. The peak at ~200 K in Fig. 2(a) cannot be explained by our calculations. The origin of this peak is unclear at present. Hot carrier effects in high electric field such as impact ionization of the deep acceptor and drift velocity overshoot might affect the temperature dependence around 200 K. The impact ionization increases the carrier density suddenly, resulting in an increase of THz radiation intensity. The drift velocity overshoot decreases the drift velocity at high electric field, which leads to a decrease of THz radiation intensity. It is reported that these effects in a quasiequilibrium state occur at the electric field of ~10 kV/cm for SI InP.[30] The calculated surface electric field is ~8 kV/cm at 200 K and this value is close to the critical value of 10 kV/cm for hot carrier effects. Therefore, there is a possibility that the increase and decrease of the THz radiation amplitude near 200 K in Fig. 2(a) can be explained by the impact ionization and the drift overshoot associated with the hot carrier effects, respectively. The THz radiation amplitude increases with increasing temperature near room temperature as shown in Fig. 2(a) and a further increase is expected at higher temperatures from our calculation. Actually, we have confirmed the enhancement of the THz radiation amplitude for SI InP above room temperature, and THz radiation intensity at ~400 K is more than three times larger than that at room temperature. Very recently, we reported the enhancement of THz intensity for SI GaAs above room temperature.[31] It was shown that the THz radiation intensity for SI GaAs at ~500 K is more than 30 times larger than that at room temperature.

The temperature T_{rev} at which the polarity reversal of THz wave forms occurs shown Figs. 1(a) and 2(a) is determined by a balance between J_{drift} and J_{diffus}. The decreases of E_s and w shown in Fig. 4 contribute to the decrease of J_{drift} with decreasing temperature. The increase of τ_e shown in Fig. 5 contributes to the increase of both J_{drift} and J_{diffus} with decreasing temperature. So we insist that the crossover of J_{drift} and J_{diffus} with temperature is mainly due to decreases of E_s and w with decreasing temperature, which are affected by the doping density and the impurity level of the deep impurity, as stated before. The surface electric field is sensitive to the surface condition because the change of the

surface condition affects the surface Fermi level. Actually, it is confirmed that T_{rev} changes by changing the surface condition with chemical etching.

It is important to point out the difference between THz radiations for *n*- and *p*-type InP and that for SI-InP. As stated before, the THz radiation for *n*- and *p*-type InP is emitted by the current surge effect at all temperatures of the measurement (10–300 K), because the magnitude of $E_s \sim 300$ kV/cm for the doping density $\sim 10^{18}$ cm^{-3} is much larger than $E_s \sim 10$ kV/cm for SI InP. However, the intensity of THz radiation for SI InP is more than 100 times stronger than that for *n*- and *p*-type InP at room temperature. This is explained by the transmittance of the THz wave at the sample surface. The transmittance of the THz wave for SI InP is much higher than that for *n*- and *p*-type InP because the high free-carrier density reduces the transmittance in the THz frequency range.

IV. CONCLUSIONS

In summary, we have observed the temperature dependence of THz radiation from SI-InP surfaces for low- and high-density excitations by ultrashort laser pulses. We show that the wave forms as well as the intensity of the THz wave change drastically by excitation conditions such as excitation power density and temperature. Reversal of polarity with temperature has been observed at ~ 140 K for low-density excitation, while the monotonical increase of the amplitude has been observed for high-density excitation with decreasing temperature. This difference of the temperature dependence is explained by the different radiation mechanisms, that is, optical rectification for high-density excitation and generation of the transient current flow by photoexcitation for low-density excitation. Polarity reversal for low-density excitation indicates the reversal of the sub-pico-second carrier transport direction, which is caused by a crossover of the radiation mechanisms associated with the drift and diffusion currents. The results of the calculation based on the drift-diffusion model support our explanation. We conclude that the dominant radiation mechanism for low-density excitation is the current surge effect due to the surface electric field at high temperatures and the photo-Dember effect at low temperatures.

ACKNOWLEDGMENTS

The authors thank T. Sugino, T. Itatani, M. Sakai, M. Tani, O. Morikawa, and A. Quema for fruitful discussions. One of the authors (M.N.) acknowledges the JSPS Research Fellowships for Young Scientists. Part of this work has been supported by the Grant-in-Aid for Scientific Research from the Ministry of Education, Culture, Sports, Science, and Technology, Japan.

*Electronic address: nak@issp.u-tokyo.ac.jp

†Present address: Laser Development Sec. Development Center, Sony Shiroishi Semiconductor Incorporated, 3-53-2 Shiratori Shiroishi-shi, Miyagi-ken, 989-0734, Japan.

[1] X.-C. Chang, B. B. Hu, J. T. Darrow, and D. H. Auston, Appl. Phys. Lett. **56**, 1011 (1990).

[2] B. B. Hu, X.-C. Zhang, and D. H. Auston, Appl. Phys. Lett. **57**, 2629 (1990).

[3] X.-C. Zhang and D. H. Auston, J. Appl. Phys. **71**, 326 (1992).

[4] X. -C. Zhang and Y. Jin, in *Perspectives in Optoelectronics*, edited by S. S. Jha (World Scientific, Singapore, 1995), pp. 81–138.

[5] M. C. Nuss, D. H. Auston, and F. Capasso, Phys. Rev. Lett. **58**, 2355 (1987).

[6] M. van Exter and D. Grischkowsky, Phys. Rev. B **41**, 12 140 (1990).

[7] B. B. Hu and M. C. Nuss, Opt. Lett. **20**, 1716 (1995).

[8] R. Huber, F. Tauser, A. Brodschelm, M. Bichler, G. Abstreiter, and A. Leitenstorfer, Nature (London) **414**, 286 (2001).

[9] B. B. Hu, E. A. Souza, W. H. Knox, J. E. Cunningham, M. C. Nuss, A. V. Kuznetzov, and S. L. Chuang, Phys. Rev. Lett. **74**, 1689 (1995).

[10] A. Leitenstorfer, S. Hunsche, J. Shah, M. C. Nuss, and W. H. Knox, Phys. Rev. B **61**, 16 642 (2000).

[11] H. Dember, Phys. Z. **32**, 554 (1931).

[12] T. Dekorsy, H. Auer, H. J. Bakker, H. G. Roskos, and H. Kurz, Phys. Rev. B **53**, 4005 (1996).

[13] M. B. Johnston, D. M. Whittaker, A. Corchia, A. G. Davies, and E. H. Linfield, Phys. Rev. B **65**, 165301 (2002).

[14] S. L. Chuang, S. Schmitt-Rink, B. I. Greene, P. N. Saeta, and A. F. J. Levi, Phys. Rev. Lett. **68**, 102 (1992).

[15] P. N. Saeta, B. I. Greene, and S. L. Chuang, Appl. Phys. Lett. **63**, 3482 (1993).

[16] S. C. Howells, S. D. Herrera, and L. A. Schlie, Appl. Phys. Lett. **65**, 2946 (1994); S. C. Howells and L. A. Schlie, *ibid.* **67**, 3688 (1995).

[17] H. Ohtake, S. Ono, Z. Liu, N. Sarukura, M. Ohta, K. Watanabe, and Y. Matsumoto, Jpn. J. Appl. Phys., Part 2 **38**, L1186 (1999).

[18] S. Kono, P. Gu, M. Tani, and K. Sakai, Appl. Phys. B: Lasers Opt. **71**, 901 (2000).

[19] *Numerical Data and Functional Relationships in Science and Technology*, edited by W. Martienssen and O. Madelung, Landolt-Börnstein, New Series, Group III, Vol. 17 (Springer, Berlin, 1982), pp. 281–297.

[20] F. W. Smith, H. Q. Le, V. Diadiuk, M. A. Hollis, A. R. Calawa, S. Gupta, M. Frankel, D. R. Dykaar, G. A. Mourou, and T. Y. Hsiang, Appl. Phys. Lett. **54**, 890 (1989).

[21] S. M. Sze, *Physics of Semiconductor Devices*, 2nd ed. (Wiley, New York, 1991).

[22] W. E. Spicer, P. W. Chye, P. R. Skeath, C. Y. Su, and I. Lindau, J. Vac. Sci. Technol. **16**, 1422 (1979); H. Hasegawa and H. Ohno, J. Vac. Sci. Technol. B **4**, 1130 (1986).

[23] T. Dekorsy, T. Pfeifer, W. Kutt, and H. Kurz, Phys. Rev. B **47**, 3842 (1993).

[24] R. Kersting, J. N. Heyman, G. Strasser, and K. Unterrainer, Phys. Rev. B **58**, 4553 (1998).

[25] S. Selberherr, *Analysis and Simulation of Semiconductor Devices* (Springer-Verlag, New York, 1984).

[26] W. H. Knox, D. S. Chemla, G. Livescu, J. E. Cunningham, and J. E. Henry, Phys. Rev. Lett. **61**, 1290 (1988).

[27] A. M. Hennel, *Properties of Indium Phosphide* (Institution of Electrical Engineers, London, 1991), p. 157.
[28] K. Fletcher and P. N. Butcher, J. Phys. C **5**, 212 (1972); C. Erginsoy, Phys. Rev. **79**, 1013 (1950).
[29] R. U. Jepsen, R. H. Jacobsen, and S. R. Keiding, J. Opt. Soc. Am. B **13**, 2424 (1996).
[30] T. Turki, G. Picoli, and J. E. Viallet, J. Appl. Phys. **73**, 8340 (1993).
[31] M. Nakajima, M. Takahashi, and M. Hangyo, Appl. Phys. Lett. **81**, 1462 (2002).